Journal of Science and Technology in Civil Engineering, NUCE 2021. 15 (3): 13–29

SHEAR STRENGTH MODEL AND PREDICTION OF FAILURE MODE FOR MULTI-SPIRAL COLUMN

Ngo Si Huy[a], Nguyen Ngoc Tan[b,*], Mai Thi Hong[a]

[a]*Department of Engineering and Technology, Hong Duc University, 565 Quang Trung Street, Dong Ve Ward, Thanh Hoa City, Vietnam*
[b]*Faculty of Building and Industrial Construction, National University of Civil Engineering, 55 Giai Phong Road, Hai Ba Trung District, Hanoi, Vietnam*

Article history:
Received 17/06/2021, Revised 22/07/2021, Accepted 23/07/2021

Abstract

The damage of reinforced concrete columns due to shear is often serious, so this type of failure should be avoided from the design. In this paper, a model derived based on the discrete computational method is proposed to calculate the shear strength of column carried by multi-spiral transverse reinforcement, accounting for the effect of compression depth. Furthermore, based on this model, a method is proposed to predict the failure mode of multi-spiral columns. The test database of multi-spiral columns from previous studies is used to validate both the shear strength and failure mode predictions. The proposed model with a crack angle of 40 degrees gives the best estimation of the shear strength of multi-spiral columns, and the proposed method predicts well the failure mode of these columns. To avoid shear failure, the ratio of the minimum shear strength calculated from the proposed model with a crack angle of 40 degrees to the shear force based on the moment-curvature analysis is suggested to be larger than 1.2.

Keywords: shear strength model; failure mode; shear failure; multi-spiral column; shear crack angle; compression depth.

https://doi.org/10.31814/stce.nuce2021-15(3)-02

1. Introduction

In reinforced concrete columns, shear failure is considered a severe failure mode that should be avoided because of its brittle nature. This mode of failure usually occurs suddenly, and it is difficult to predict, leading to serious damage to building structures and hard to repair. Therefore, all columns should be designed as ductile concrete members, which can suffer a large deformation and survive during a strong earthquake. Conventionally, shear force corresponding to flexural strength has to be less than the shear strength capacity of columns. Hence, accurate determination of the shear resistance capacity of reinforced concrete columns plays an important role in structure design, especially for a new structure such as multi-spiral columns.

The type of transverse reinforcement is an aspect that has a significant influence on the performance of reinforced concrete columns [1, 2]. As basic knowledge, the superior confinement of spiral transverse reinforcement (Fig. 1(b)) to that of conventional tied reinforcement (Fig. 1(a)) has been stated in reinforced concrete textbooks [3, 4]. Based on that, the innovation of spiral transverse reinforcement schemes has been attracted to many researchers over the world, especially for

*Corresponding author. *E-mail address:* tannn@nuce.edu.vn (Tan, N. N.)

other cross-sections than circular shapes. In which the two-spiral (Fig. 1(c)), which was developed from single-spiral (Fig. 1(b)) by adding one more spiral for oblong cross-section, was first studied by many researchers [5–11]. In order to reduce spiral size for large bridge columns and apply automation construction technology in the production of spiral reinforcement, Ou et al. [8, 12] have proposed seven-spiral for oblong columns (Fig. 1(d)). Test results from previous studies indicated that even with less amount of transverse reinforcement, two-spiral and seven-spiral columns exhibited comparable or even better seismic performance than the corresponding conventional tied columns.

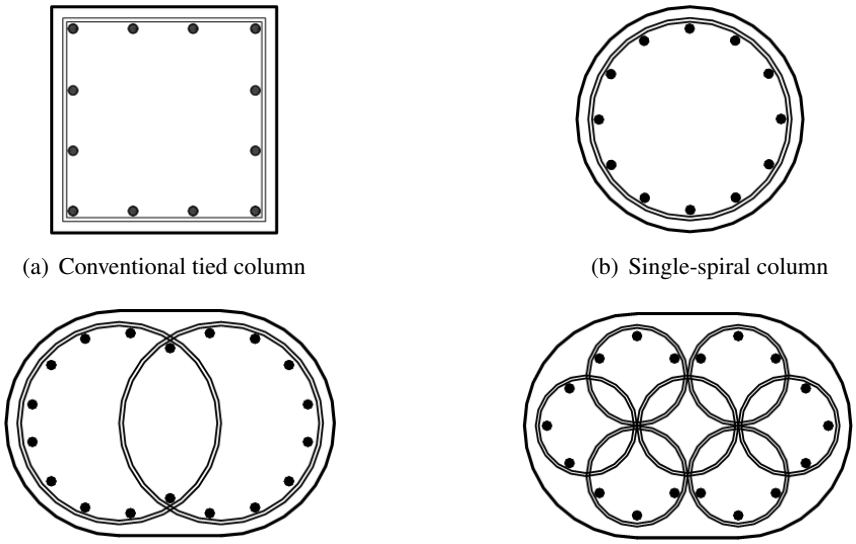

(a) Conventional tied column (b) Single-spiral column

(c) Two-spiral column (d) Seven-spiral column

Figure 1. Cross-section of different types of columns

Recently, Yin et al. [1] have proposed five-spiral transverse reinforcement (Fig. 2(a)) for square columns by adding four small spirals at the corner of the single spiral. Based on uniaxial compressive loading, the square five-spiral column showed higher strength and ductility than a corresponding column with conventional tied transverse reinforcement. Similarly, Wu et al. [10] and Ou et al. [12] have developed innovative six-spiral and eleven-spiral for rectangular columns by adding four small spirals at the corners of two-spiral and seven-spiral as shown in Figs. 2(b) and 2(c), respectively.

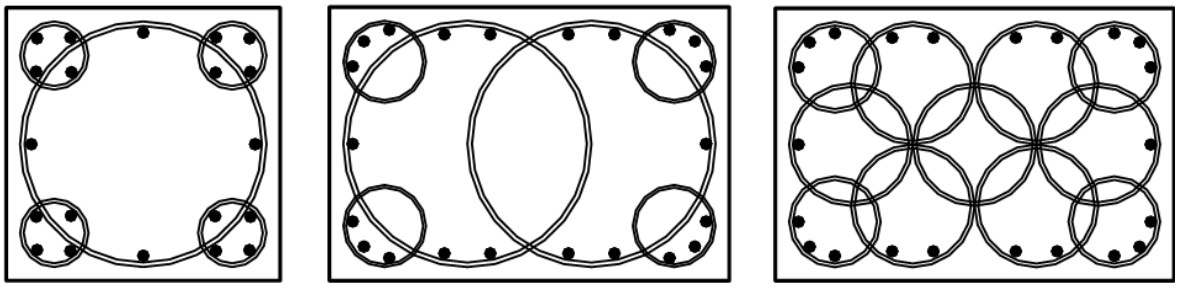

(a) Five-spiral column (b) Six-spiral column (c) Eleven-spiral column

Figure 2. Square and rectangular cross-section of multi-spiralcolumns

For lateral cyclic loading tests, the better performance of six-spiral and eleven-spiral columns than those of tied columns has been reported in previous studies even with less amount of transverse reinforcement [10, 12]. In Vietnam, the use of spiral transverse reinforcement for circular columns under axial loading has just been studied by Nguyen and Pham [13].

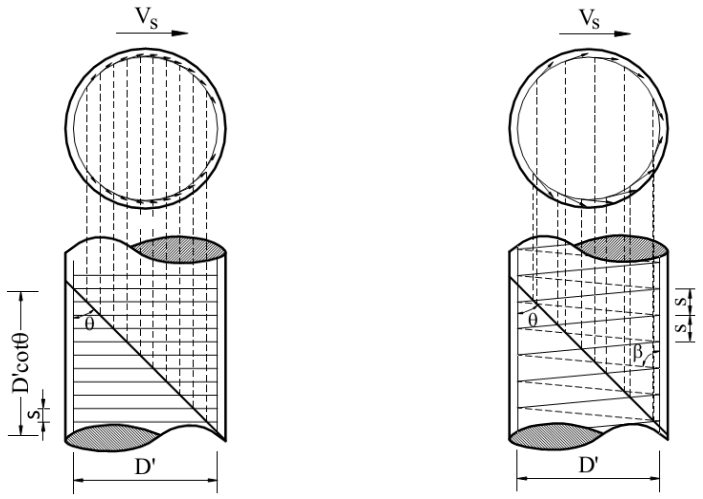

(a) Single-circular hoop (b) Single-spiral stirrups

Figure 3. Shear strength carried by different types of transverse reinforcement

The shear strength carried by a single-circular hoop was first derived by Ang et al. [14], as shown in Fig. 3(a) and Eq. (1) based on the assumptions that the spacing between hoops (s) is very small. In American standards such as AASHTO (2011) [15] and Caltrans SDC (2019) [16], Eq. (2) is used to calculate the shear strength provided by multi-circular hoops or multi-spiral transverse reinforcement. It is noticed that Eq. (2) is a form of Eq. (1) with assuming that the shear strength of multi-circular hoops or multi-spiral equals the sum of shear strength provided by each circular-hoop or spiral and the shear crack angle (θ) is equal to 45 degrees. When calculation shear strength for oblong two-spiral columns, Tanaka and Park [11] used Eq. (2) with $n = 2$. It is noticed that the shear strength provided by a circular hoop and a spiral reinforcement is different, as shown in Fig. 3. Moreover, most columns failed by shear often have large spiral spacing, hence using Eq. (1) or Eq. (2) to calculate the shear strength of these columns results in high non-conservatism. Previous studies have pointed out that the use of Eqs. (1) or (2) for spiral transverse reinforcement led to the high error, especially with $s/(D' \cot\theta) \geq 0.2$ [17–19]. Recently, Ou and Ngo [20, 21] have developed shear strength models for multi-spiral columns. These models were derived based on the discrete computational method and intersection points between shear crack and circular-hoop or spiral reinforcement. The difference between shear strength of circular-hoop and spiral transverse reinforcement was clarified in their models. They also pointed out that the use of Eq. (2) to calculate the shear strength of spiral transverse reinforcement leads to a high error, especially with a high ratio between spiral spacing and diameter of spiral. However, their models do not consider the effect of compression zone, and transverse reinforcement within this region does not contribute to the shear strength.

$$V_s = \frac{\pi}{2} A_{sh} f_{yh} \frac{D' \cot\theta}{s} \tag{1}$$

$$V_s = \frac{A_v f_{yh} D'}{s}, \quad \text{where } A_v = n\left(\frac{\pi}{2}\right) A_{sh} \tag{2}$$

in which V_s is shear strength provided by transverse reinforcement, A_{sh} is the cross-sectional area of a transverse reinforcing bar, f_{yh} is the yield strength of transverse reinforcement, D' is the diameter of a circular hoop or spiral, s is the regular spacing of transverse reinforcements, θ is the angle between a shear crack and the longitudinal axis of the column, A_v is the total area of transverse reinforcement, and n is the number of circular-hoop series or spirals.

The shear strength model is an important tool to assess the shear behavior of columns. However, most of the existed shear strength models have been developed for conventional columns with tied transverse reinforcement [22–24]. For spiral columns, Kowalsky and Priestley [25] have developed a shear strength model for single-spiral columns based on Priestley's model [22]. However, that model still used the form of Eq. (1) to calculate the shear strength of single-spiral, even that equation is the shear strength of a single-circular hoop. Therefore, developing an assessment shear strength model for multi-spiral columns considering the effect of compression zone is an objective of the present study. Based on this model, a simple method to predict the failure mode of multi-spiral columns is also developed.

2. Shear strength model for multi-spiral columns

2.1. Proposed shear strength model for multi-spiral columns

Priestley et al. [22] proposed the shear strength model for conventional tied columns as shown in Eq. (3). In which the shear strength carried by concrete (V_c), the shear strength enhancement by axial load (V_a), and the shear strength carried by transverse reinforcement are calculated based on Eqs. (4) – (6). In Eq. (4), k is a reduction factor, which reduces from 0.29 to 0.1 when the column displacement ductility increases from 2 to 4. It is noticed that Eq. (6) is used to calculate the shear strength provided by conventional tied transverse reinforcement, and it does not include the effect of the compression zone. Transverse reinforcement in the compression zone does not contribute to the shear resistance of the column [25]. The present study proposes a model to assess the shear strength for multi-spiral columns based on Eq. (3). In which, the shear strength carried by concrete and the shear strength enhancement by the axial load is kept as the original model proposed by Priestley et al. [22]. Eq. (6) will be replaced by another equation to calculate the shear strength provided by multi-spiral transverse reinforcement considering the effect of the compression zone, which will be derived later.

$$V_n = V_c + V_s + V_a \tag{3}$$

$$V_c = k\sqrt{f'_c} \times 0.8A_g \tag{4}$$

$$V_a = P\tan\theta = \frac{D-c}{L}P \tag{5}$$

$$V_s = \frac{A_{sh} f_{yh} D'}{s}\cot 30^\circ \tag{6}$$

where V_n is the column shear capacity, V_c is the shear strength provided by concrete, V_s is the shear strength provided by transverse reinforcement, V_a is the shear strength enhancement by axial load, A_g is the gross area of the section, f'_c is the concrete compressive strength, D is the width of cross-section, c is the compression depth of cross-section, L is the effective column height, P is the axial force (positive for compression), θ is the angle between a shear crack and the longitudinal axis of

the column, A_{sh} is the cross-sectional area of transverse reinforcement, f_{yh} is the yield strength of transverse reinforcement, s is the spacing of transverse reinforcement, and D' is the distance between centers of the peripheral hoop or spiral.

2.2. Shear strength provided by single spiral reinforcement

The general shear strength model for single-spiral transverse reinforcement is proposed by Ou and Ngo [20, 21], but that model does not consider the effect of compression zone. In this section, a general model for single-spiral transverse reinforcement considering the effect of compression zone is developed based on the model proposed by Ou and Ngo [20]. The shear strength provided by single spiral reinforcement is calculated by summing the shear resistance from all intersection points between shear crack and transverse reinforcement as Eq. (7). As shown in Fig. 4, a Cartesian coordinate system is used to determine the intersection points. The dashed and solid lines represent half of the spiral on the back and front sides of the column, respectively. Based on the coordinate system, the equation for the back side and front side spiral lines of the *i*th spiral level are shown in Eqs. (8) and (9), respectively. The function of the critical shear crack can be represented by Eq. (10).

$$V_s = A_{sh} f_{yh} \sin\beta \sum_i \left(\sin\alpha_i^1 + \sin\alpha_i^2\right) \tag{7}$$

$$y = \frac{s}{2D'}\mathrm{x} + s\left(i - \frac{l}{2D'}\right) \tag{8}$$

$$y = -\frac{s}{2D'}\mathrm{x} + s\left(i + 1 + \frac{l}{2D'}\right) \tag{9}$$

$$y = x\cot\theta \tag{10}$$

The X coordinate of the intersection points between the crack and the spiral lines of the i^{th} spiral level can be derived by solving the Eqs. (11) and (12). Because shear cannot transfer through the compression zone (as seen in Fig. 4), hence $l \le x_i^1, x_i^2 \le l + D' - c'$, the range of i is shown in Eqs. (13) and (14).

$$x_i^1 = \frac{s(i-b)}{a_1} \text{ from } \begin{cases} y = x\cot\theta \\ y = \dfrac{s}{2D'}x + s\left(i - \dfrac{l}{2D'}\right) \end{cases} \tag{11}$$

$$x_i^2 = \frac{s(i+1+b)}{a_2} \text{ from } \begin{cases} y = x\cot\theta \\ y = -\dfrac{s}{2D'}x + s\left(i + 1 + \dfrac{l}{2D'}\right) \end{cases} \tag{12}$$

where $b = l/2D'$, $a_1 = \cot\theta - s/2D'$, $a_2 = \cot\theta + s/2D'$.

$$N_l \le i \le N_l + N_{D'} - N_{c'} - 0.5 + \frac{c'}{2D'} \text{ for } x_i^1 \tag{13}$$

$$N_l - 1 \le i \le N_l + N_{D'} - N_{c'} - 0.5 - \frac{c'}{2D'} \text{ for } x_i^2 \tag{14}$$

where $N_l = \dfrac{l}{s}\cot\theta, N_{D'} = \dfrac{D'}{s}\cot\theta$; and $N_{c'} = \dfrac{c'}{s}\cot\theta$.

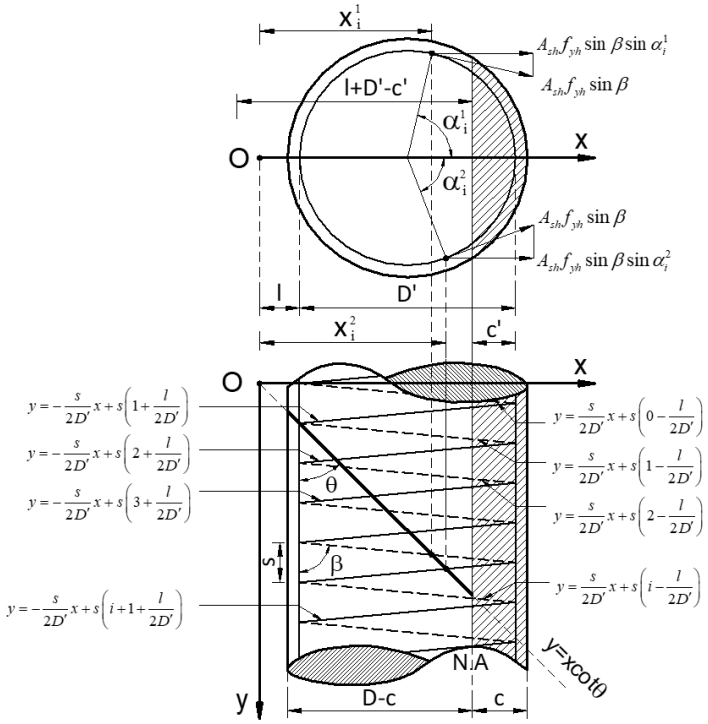

Figure 4. Shear strength provided by single-spiral transverse reinforcement

It is noticed that i should be an integer, therefore:

$$\text{int}\left[N_l\right] + 1 \le i \le \text{int}\left[N_l + N_{D'} - N_{c'} - 0.5 + \frac{c'}{2D'}\right] \text{ for } x_i^1 \tag{15}$$

$$\text{int}\left[N_l\right] \le i \le \text{int}\left[N_l + N_{D'} - N_{c'} - 0.5 - \frac{c'}{2D'}\right] \text{ for } x_i^2 \tag{16}$$

$\sin\alpha_i^1$ and $\sin\alpha_i^2$ in Eq. (7) can be calculated based on Ou and Ngo's equations, which are expressed as Eqs. (17) and (18).

$$\sin\alpha_i^1 = \sqrt{1-\cos^2\alpha_i^1} = \sqrt{1-\left(\frac{l+0.5D'-x_i^1}{0.5D'}\right)^2} = \sqrt{1-\left(\frac{N_l+0.5N_{D'}-\frac{i-b}{a_1}\cot\theta}{0.5N_{D'}}\right)^2} \tag{17}$$

$$\sin\alpha_i^2 = \sqrt{1-\cos^2\alpha_i^2} = \sqrt{1-\left(\frac{l+0.5D'-x_i^2}{0.5D'}\right)^2} = \sqrt{1-\left(\frac{N_l+0.5N_{D'}-\frac{i+1+b}{a_2}\cot\theta}{0.5N_{D'}}\right)^2} \tag{18}$$

Substituting Eqs. (17) and (18) into Eq. (7), the shear resistance provided single-spiral transverse reinforcement is calculated by Eq. (19).

$$V_l^{c'} = A_{sh}f_{yh}\sin\beta\left[\sum_{i=\text{int}[N_l]+1}^{\text{int}\left[N_l+N_{D'}-N_{c'}-0.5+c'/D'\right]}\sqrt{1-\left(\frac{N_l+0.5N_{D'}-\frac{i-b}{a_1}\cot\theta}{0.5N_{D'}}\right)^2} + \sum_{i=\text{int}[N_l]}^{\text{int}\left[N_l+N_{D'}-N_{c'}-0.5-c'/D'\right]}\sqrt{1-\left(\frac{N_l+0.5N_{D'}-\frac{i+1+b}{a_2}\cot\theta}{0.5N_{D'}}\right)^2}\right] \tag{19}$$

where, subscript l denotes the distance from the origin to the first edge of the spiral, superscript c' denotes the distance from the neutral axis to the edge of the spiral in the compression zone as shown in Fig. 4. It is noticed that for multi-spiral transverse reinforcement, each spiral has its own location and compression zone corresponding to each value of l and c'. Eq. (19) is the general model to calculate the shear strength carried by single-spiral transverse reinforcement, which is applicable to any shear crack angle (by adjusting θ), any compression depth (by adjusting c'), and any location of the shear crack (by adjusting l).

2.3. Shear strength provided by multi-spiral reinforcement

For multi-spiral transverse reinforcement, the model is the superposition of single-spiral with an assumption that each spiral works effectively and can be accounted as independent single-spiral, as shown in Eq. (20). In which, shear strength provided by each spiral is calculated by Eq. (19). In previous studies, Ou and Ngo [20, 21] have indicated that the shear crack, which intercepts the edges of spirals, is a potential critical shear crack, leading to the smallest shear strength capacity. For simply, assuming that the shear crack is starting from the edge of the first spiral as shown in Fig. 5. As examples, the models for seven-spiral under strong axis bending, and seven-spiral under weak axis bending are shown in Eqs. (21) and (22), respectively. In Eq. (21), the distance from the origin to the first edge of first, second, third, fourth, fifth, sixth, and seventh spirals are $l_1 = 0$, $l_2 = l_3$, l_4, $l_5 = l_6$ and l_7, respectively. Their corresponding compression depths are $c'_1 = c'_2 = c'_3 = c'_4 = 0, c'_5 = c'_6$ and c'_7. Similarly, the value of l_j and c'_j for seven-spiral under weak axis bending are illustrated in Fig. 5(b), with $l_1 = l_2 = 0$, $l_3 = l_4 = l_5$, $l_6 = l_7$ and $c'_1 = c'_2 = c'_3 = c'_4 = c'_5 = 0, c'_6 = c'_7$.

$$V_s = \sum_j V_{l_j}^{c'_j} \tag{20}$$

where j is the spiral number; c'_j is the compression depth in the j^{th} spiral; l_j is the distance from the origin to the first edge of j^{th} spiral.

$$V_{\text{Seven}}^{\text{Strong}} = V_0^0 + 2V_{l_2}^0 + V_{l_3}^0 + 2V_{l_4}^{c'_4} + V_{l_5}^{c'_5} \tag{21}$$

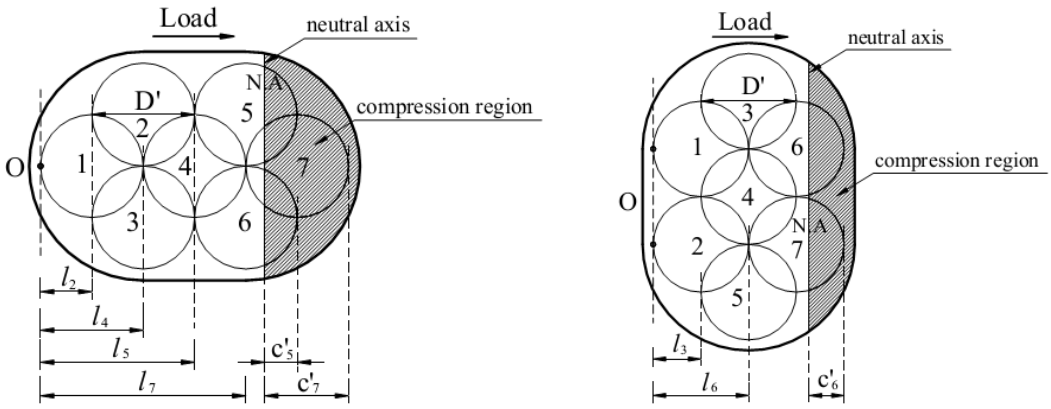

(a) Strong axis bending (b) Weak axis bending

Figure 5. Cross-section of a seven-spiral column under strong/weak axis bending

$$V_{\text{Seven}}^{\text{Weak}} = 2V_0^0 + 3V_{l_2}^0 + 2V_{l_3}^{c'_3} \tag{22}$$

Based on the superposition method (Eq. (20)) and general model for single-spiral (Eq. (19)), the models for any multi-spiral can be derived. It is noticed that these models (Eqs. (21)–(22)) reflect the different behavior of spirals even they are in the same cross-section and the different shear resistance of columns under varying direction loading. These factors are not considered in Eq. (2).

3. Comparison of model with column database

3.1. Column database

The database of 29 multi-spiral columns is shown in Table 1. In which 18 columns were failed by shear, they are used for shear strength comparison obtained from the experiment and the model. 11 later columns were failed by flexure, and they are used to predict the failure mode. Material properties and other important parameters of these columns are listed in Table 1. More details about specimen design and test results of all columns presented herein can be found in the references [5–12]. It is

Table 1. Test database of multi-spiral columns

No.	Column name	$\frac{P}{A_g f_c'}$	A_g (mm^2)	L (mm)	f_c' (MPa)	Longitudinal steel		Transverse reinforcement			θ	Failure mode
						Details	f_y (MPa)	d_t (mm)	s (mm)	f_{yh} (MPa)		
1	Inter 1 [5]	0.02	220000	1220	35	30D16	442	6.35	89	448	35	Shear
2	Inter 2 [5]	-0.1	220000	1220	34	30D16	442	6.35	89	448	35	Shear
3	Inter 3 [5]	0.35	220000	1220	35	30D16	442	6.35	89	448	35	Shear
4	Inter 4-C [5]	0.35	220000	1220	37	30D16	442	6.35	89	448	35	Shear
5	Inter 4-T [5]	-0.1	220000	1220	37	30D16	442	6.35	89	448	35	Shear
6	ISH1.0 [6]	0.1	79627	737	34	32D10	443	4.05	38	466	45	Shear
7	ISH1.25 [6]	0.07	86993	800	50	34D10	431	4.05	25	449	45	Shear
8	ISH1.5 [6]	0.08	94105	877	34	38D10	443	4.05	25	467	45	Shear
9	ISH1.5T [6]	0.07	94105	877	50	38D10	431	4.05	25	456	45	Shear
10	Column 1 [7]	0.09	85509	1219	32	14D16	420	6.35	127	420*	35	Shear
11	Column 3 [7]	0.09	93251	1219	32	14D16	420	6.35	127	420*	38	Shear
12	Column 4 [7]	0.09	85509	1219	32	10D16 4D6	420	6.35	127	420*	35	Shear
13	DM1R-SL [8]	0.06	444743	1580	64	20D32	468	10	120	605	42	Shear
14	DM1R-SS [8]	0.06	444743	1200	70	20D32	468	10	100	605	37	Shear
15	DM2R-SL [8]	0.07	444743	1580	58	14D32 8D29	468 479	8	120	648	35	Shear
16	DM2R-SS [8]	0.06	444743	1200	69	14D32 8D29	468 479	8	100	648	42	Shear
17	DM2RI-SS [8]	0.07	444743	1200	55	20D32	468	8	80	648	34	Shear
18	Unit 6 [9]	0.05	432743	1620	31	36D13	386	6	200	364	31	Shear
19	Unit 4 [9]	0.05	432743	1620	31	36D13	386	6	50	364	NA	Flexure
20	Unit 5 [9]	0.05	432743	1620	29	36D13	386	6	100	364	NA	Flexure
21	DM-CS [10]	0.1	444743	2100	44	18D25	469	10	60	605	NA	Flexure
22	DM-CW [10]	0.1	444743	2100	54	18D25	469	10	60	605	NA	Flexure
23	CM-CW [10]	0.1	522000	2100	43	22D25	469	10 6	60 60	605 581	NA	Flexure
24	Unit 10 [11]	0.1	205664	1784	21	14D20	485	10	80	308	NA	Flexure
25	Unit 11 [11]	0.3	205664	1784	30	14D20	485	10	100	308	NA	Flexure
26	Unit 12 [11]	0.5	205664	1784	25	14D20	485	10	75	308	NA	Flexure
27	DMR1 [12]	0.1	444743	2100	56	18D25	469	8	60	648	NA	Flexure
28	DMR2 [12]	0.1	444743	2100	47.1	6D36 12D19	484 469	8	60	648	NA	Flexure
29	CMR1 [12]	0.1	444743	2100	45.5	22D25	469	8	60	648	NA	Flexure

where, d_t is the diameter of a transverse reinforcing bar. NA means that no value is available.

noticed that the properties of materials in Table 1 are actual strengths. Only yield strengths of longitudinal and transverse reinforcement of Columns 1, 3, and 4 are specified values since their actual values were missed in its reference [7]. The compression depth of each cross-section was determined using moment-curvature analysis. The interaction between shear strength from experiment and model is shown in Fig. 6. The ratio of shear strength from the experiment to shear strength from the model ($V_{\text{exp}}/V_{\text{mod}}$) corresponding to the failure point is used to validate the proposed model in this study.

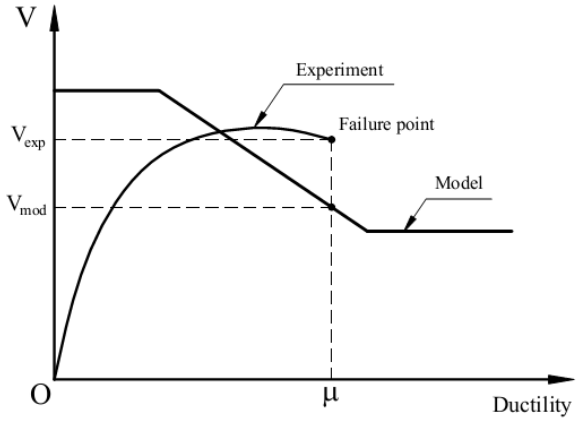

Figure 6. Illustration of shear strength from experiment and model

3.2. Effect of shear crack angle on the shear strength of columns

As in previous models [22–24], the proposed model in this study is used to assess the shear behavior of multi-spiral columns, hence the shear crack angle should be predicted first. Each model used its shear crack angle, for example, a crack angle of 45 degrees is used in Sezen' model [23], while that of 30 degrees is used in Priestley's model [22] and Aschheim's model [24]. The comparison between shear strength from the experiment and shear strength from the proposed model with the crack angles of 30, 35, 40, and 45 degrees are shown in Fig. 7. In which the lateral load is normalized by peak load for all columns to uniform evaluation. It is noticed that the shear strength capacity of columns decreases with increasing displacement ductility due to the widening of cracks in the tension region, which results in a reduction in shear strength carried by concrete (as shown in Eq. (4)). As shown in Fig. 7, the shear strength of the column is reduced with increasing crack angle. This is due to the number of intersection points between shear crack and spiral transverse reinforcement reduces since the crack angle increases. In general, the model shear strength with a crack angle of 30 degrees is often much higher than the shear strength from the experiment, while model shear strength with a crack angle of 45 degrees is often lower than that from the experiment. This is because the actual shear crack angle obtained from the experiment ranged from 31 to 45 degrees with an average value of 38.4 degrees (Table 1).

Fig. 8 shows the results of V_{exp}/V_{mod} against an arbitrary test number and crack angles. According to Fig. 8, the predicted shear strength based on 30 and 35 degrees results in much higher than experimental strength, while an adverse trend is observed with a crack angle of 45 degrees. With a crack angle of 40 degrees, the value of V_{exp}/V_{mod} is scattered around unity. The statistical results of the effect of crack angle on shear strength are presented in Table 2. The proposed model with a crack angle of 40 degrees gives the best result with a mean value of 1.03 and derivation of 0.15. It is noticed

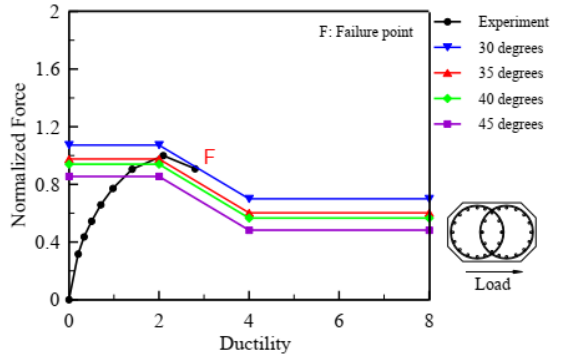

(a) Inter 1

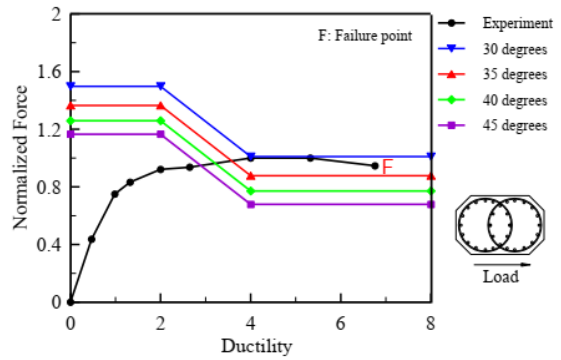

(b) Inter 2

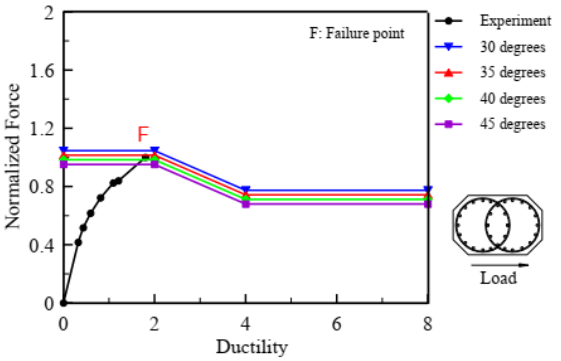

(c) Inter 3

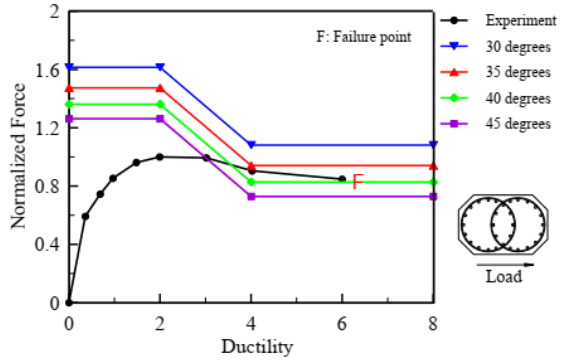

(d) Inter 4-compression

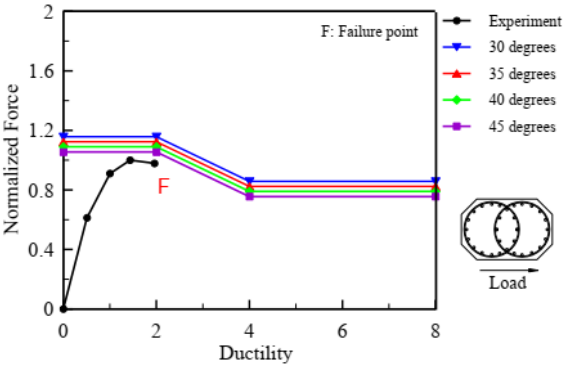

(e) Inter 4-tension

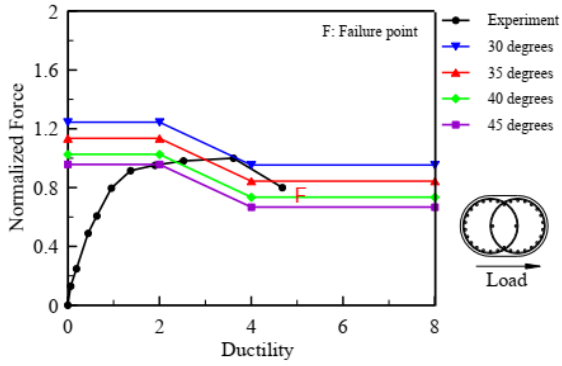

(f) ISH1.0

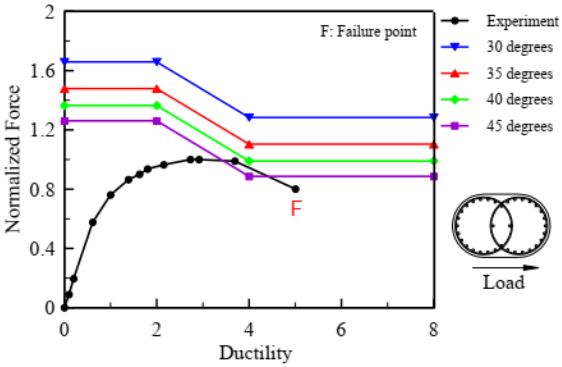

(g) ISH 1.25

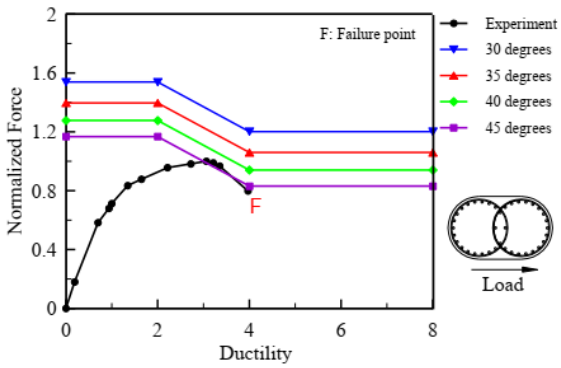

(h) ISH1.5

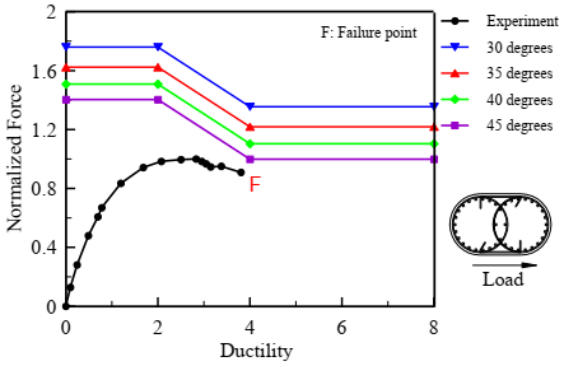

(i) ISH1.5T

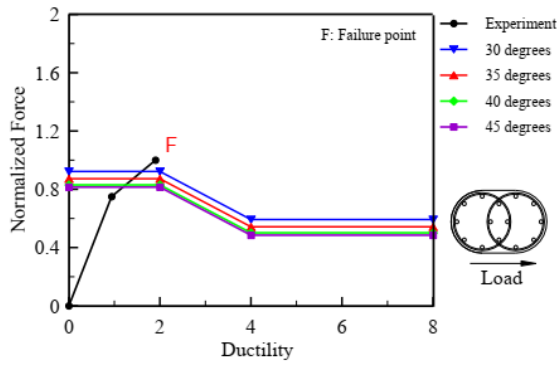

(j) Column 1

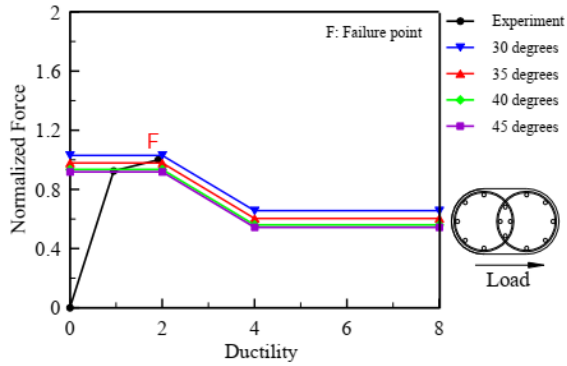

(k) Column 3

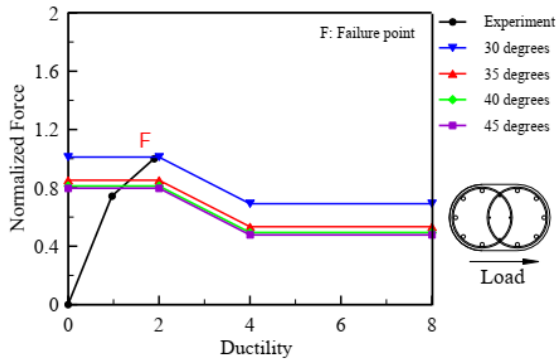

(l) Column 4

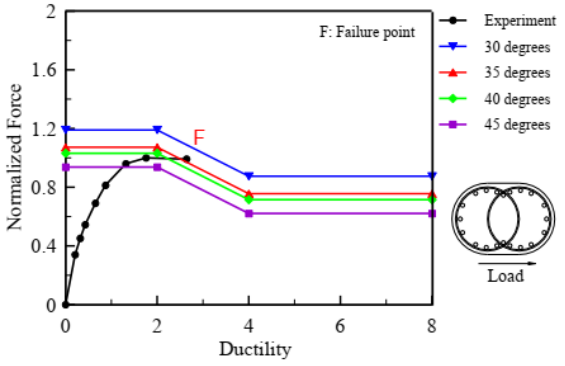

(m) DM1R-SL

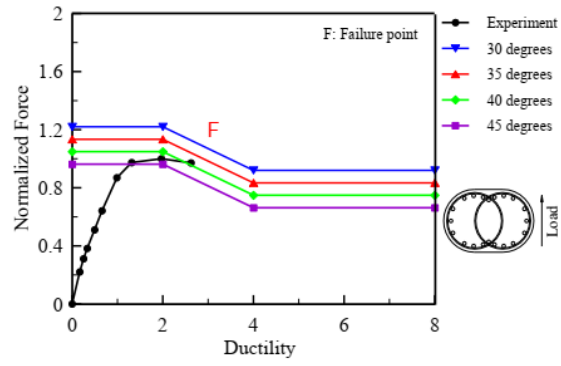

(n) DM1R-SS

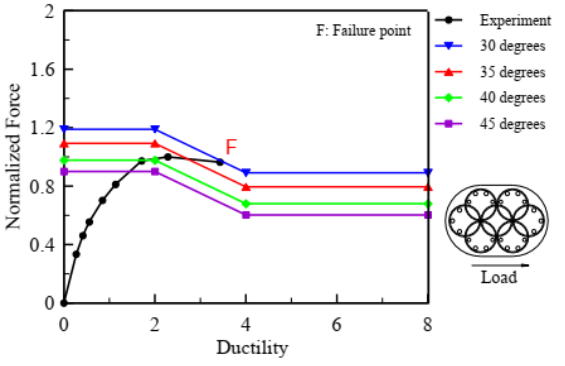

(o) DM2R-SL

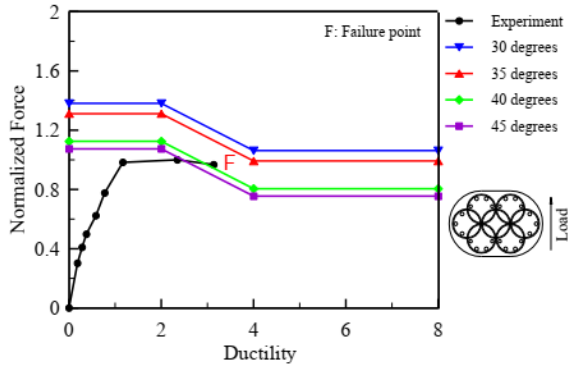

(p) DM2R-SS

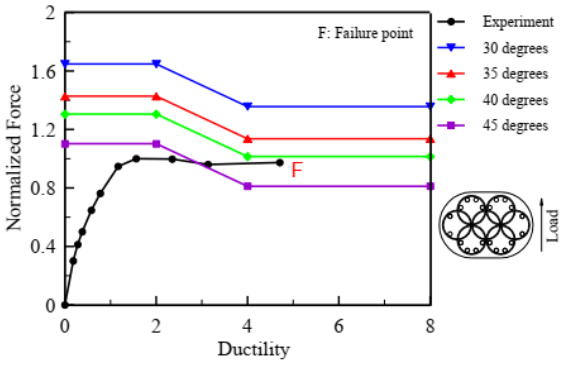

(q) DM2RI-SS

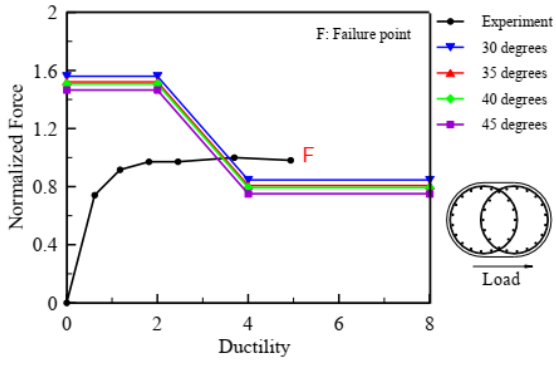

(r) Unit 6

Figure 7. Effect of shear crack angle on shear strength

that the average value of actual shear crack angles obtained from the experiment is 38.4 degrees, approximation to 40 degrees as aforementioned. This is explained why the proposed model with a crack angle of 40 degrees yields the best estimation of the shear strength of multi-spiral columns.

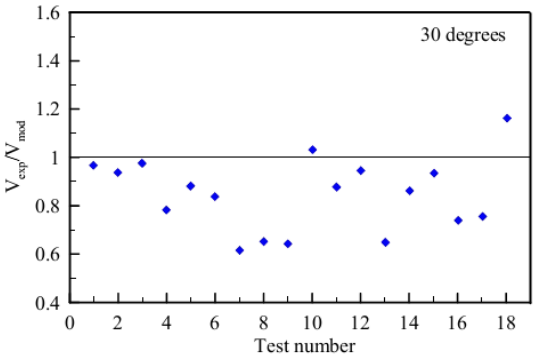

(a) 30 degrees

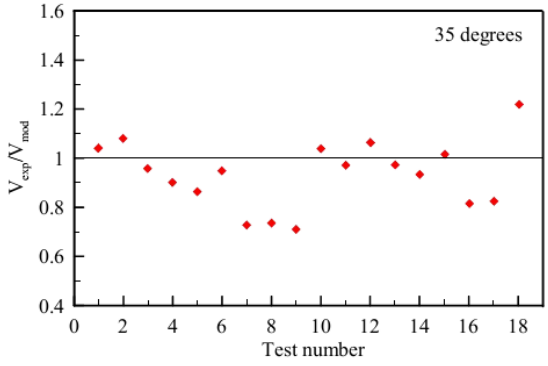

(b) 35 degrees

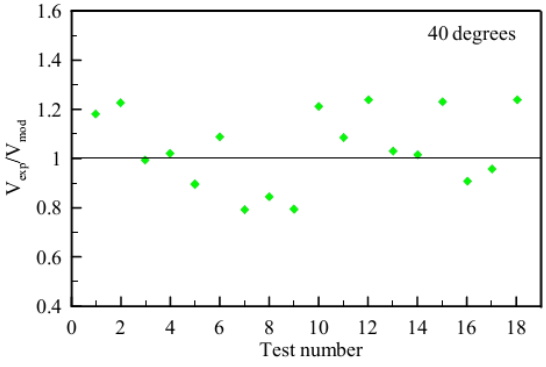

(c) 40 degrees

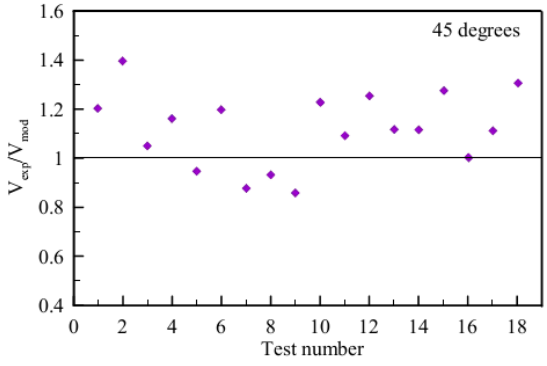

(d) 45 degrees

Figure 8. Effect of shear crack angle on shear strength

Table 2. Statistical results for the effect of shear crack angle

Crack angle	30 degrees	35 degrees	40 degrees	45 degrees
Mean and derivation	0.85 ± 0.15	0.93 ± 0.13	1.03 ± 0.15	1.11 ± 0.15

4. Prediction of column failure mode

As aforementioned, shear failure mode must be avoided during the design process because of dangerous damage. Sometimes, the prediction of failure mode is more important than the exact estimation of shear strength. In this section, a simple method is suggested to predict the failure mode of multi-spiral columns. It is noticed that the maximum lateral load can be predicted using moment-curvature analysis. The ratio of maximum lateral load from the experiment ($V_{\text{exp}}^{\text{max}}$) to maximum lateral load from moment-curvature analysis ($V_{\text{analysis}}^{\text{max}}$) of 29 multi-spiral columns presented in Table 1 is plotted in Fig. 9. Most values of $\xi = V_{\text{exp}}^{\text{max}}/V_{\text{analysis}}^{\text{max}}$ are ranged from 1.0 to 1.2. It is noticed that these values of Columns 1, 3, and 4 are significantly higher than 1.2. This is due to the use of specified material strength in the moment-curvature analysis for these columns, while other columns are analyzed with actual material strength. It means that if the actual material strength is used, the ξ values of Columns 1, 3, and 4 should be less than 1.2. In other words, the maximum probable lateral strength of multi-spiral columns is assumed to be 1.2 times maximum lateral force from moment-curvature analysis for conservatism.

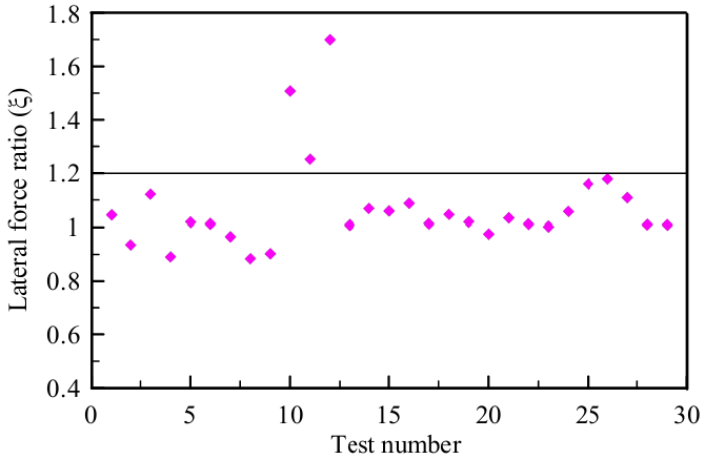

Figure 9. Ratios of maximum experimental lateral load to maximum analytical lateral load versus test number

Fig. 10 shows the theory to predict the failure mode of reinforced concrete columns. The maximum shear force corresponding to flexural strength is determined by moment-curvature analysis $V_{\text{analysis}}^{\text{max}} = M_{\text{max}}/L$ and the maximum probable shear force is assumed to be $1.2V_{\text{analysis}}^{\text{max}}$. Thus, if the minimum shear strength of column ($V_{\text{mod}}^{\text{min}}$) is higher than the maximum probable shear force (as seen in Fig. 10(a)), the column is failed by flexure. On the contrary, if the maximum shear force ($V_{\text{analysis}}^{\text{max}}$) is higher than the minimum shear strength (Fig. 10(b)), the column will be failed by shear. These findings are interpreted by two conditions as follows:

The column will be failed by flexure if

$$\frac{V_{\text{mod}}^{\text{min}}}{V_{\text{analysis}}^{\text{max}}} > 1.2 \tag{23}$$

The column will be failed by shear if

$$\frac{V_{\text{mod}}^{\text{min}}}{V_{\text{analysis}}^{\text{max}}} < 1 \tag{24}$$

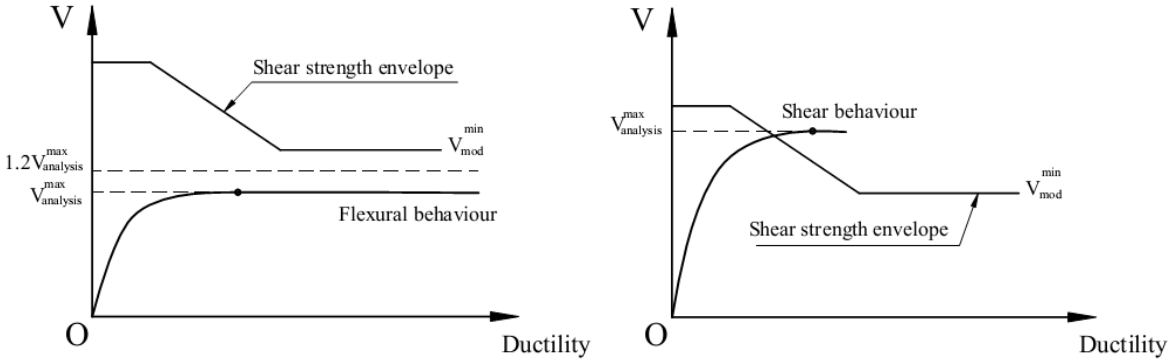

(a) Flexural failure (b) Shear failure

Figure 10. Prediction of flexural and shear failure mode

It is noticed that $V_{\text{mod}}^{\text{min}}$ is determined using the proposed model with a crack angle of 40 degrees, as aforementioned. Based on Eqs. (23) and (24), the condition to determine the column failed by shear or flexure is listed as follows (as illustrated in Fig. 11). If $1 \leq \frac{V_{\text{mod}}^{\text{min}}}{V_{\text{analysis}}^{\text{max}}} \leq 1.2$, the columns may be failed by shear or flexure.

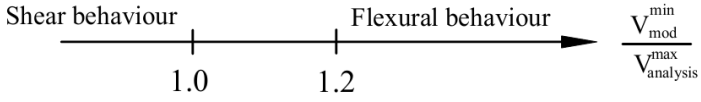

Figure 11. Determining the failure mode based on $V_{\text{mod}}^{\text{min}}/V_{\text{analysis}}^{\text{max}}$

A total of 29 multi-spiral columns failed by shear and flexure, as presented in Table 1, is used to validate the proposed failure mode prediction method. The results are presented in Table 3. As seen in Table 3, the proposed method exactly predicted failure mode for 17 of 18 columns failed by shear with $V_{\text{mod}}^{\text{min}}/V_{\text{analysis}}^{\text{max}} < 1$. Only column DM2RI-SS has $1 < V_{\text{mod}}^{\text{min}}/V_{\text{analysis}}^{\text{max}} = 1.03 < 1.2$ is not known failed by shear or flexure. This column is stated failed by shear, but its lateral displacement ductility is 4.7. Therefore, its failure mode is between flexure and shear is reasonable.

Meanwhile, for 11 columns that failed by flexure, the proposed method exactly predicts nine columns, except Unit 5 and Unit 11. As a test result, Unit 5 was considered to fail by flexural, but

Table 3. Prediction of failure mode for multi-spiral columns

No.	Column name	Actual failure mode	$\frac{V_{\text{mod}}^{\text{min}}}{V_{\text{analysis}}^{\text{max}}}$	Predicted failure mode
1	Inter 1	Shear	0.57	Shear
2	Inter 2	Shear	0.72	Shear
3	Inter 3	Shear	0.82	Shear
4	Inter 4-C	Shear	0.74	Shear
5	Inter 4-T	Shear	0.83	Shear
6	ISH1.0	Shear	0.76	Shear
7	ISH1.25	Shear	0.97	Shear
8	ISH1.5	Shear	0.83	Shear
9	ISH1.5T	Shear	0.99	Shear
10	Column 1	Shear	0.75	Shear
11	Column 3	Shear	0.68	Shear
12	Column 4	Shear	0.83	Shear
13	DM1R-SL	Shear	0.75	Shear
14	DM1R-SS	Shear	0.80	Shear
15	DM2R-SL	Shear	0.74	Shear
16	DM2R-SS	Shear	0.99	Shear
17	DM2RI-SS	Shear	1.03	Flexural-Shear
18	Unit 6	Shear	0.83	Shear
19	Unit 4	Flexure	1.30	Flexure
20	Unit 5	Flexure	0.96	Shear
21	DM-CS	Flexure	1.77	Flexure
22	DM-CW	Flexure	2.42	Flexure
23	CM-CW	Flexure	1.88	Flexure
24	Unit 10	Flexure	1.31	Flexure
25	Unit 11	Flexure	1.16	Flexural-Shear
26	Unit 12	Flexure	1.24	Flexure
27	DMR1	Flexure	3.11	Flexure
28	DMR2	Flexure	2.53	Flexure
29	CMR1	Flexure	2.65	Flexure

$V_{\text{mod}}^{\text{min}}/V_{\text{analysis}}^{\text{max}} = 0.96$ is close to unity, and its displacement ductility is 5.2. Therefore, although flexural behavior is dominated but the shear damage is also affected by the failure mode of this column. For Unit 11, which is not classified based on the proposed method, $V_{\text{mod}}^{\text{min}}/V_{\text{analysis}}^{\text{max}} = 1.16$ close to 1.2 and displacement ductility of 10 indicates that the flexural-dominated is the behavior of this column. All these findings proved that the proposed method could almost exactly predict the failure mode of multi-spiral columns. For structural engineers, the $V_{\text{mod}}^{\text{min}}/V_{\text{analysis}}^{\text{max}}$ is recommended to be larger than 1.2 in order to avoid shear damage.

5. Conclusions

This paper proposes a model to calculate the shear strength of multi-spiral columns considering the effect of the compression zone. Based on that, the model to predict the failure mode of multi-spiral columns is also proposed. The main conclusions are summarized as follows:

- A model to calculate the shear strength of column provided by multi-spiral transverse reinforcement is proposed based on a discrete computational method. This model considers the effects of shear crack angle, compression zone, the direction of loading, and the crack location.

- The proposed shear strength model with a crack angle of 40 degrees yields the best simulation shear strength of multi-spiral columns.

- The failure mode of multi-spiral columns can be predicted using the proposed shear strength model with a crack angle of 40 degrees combined with flexural strength from the moment-curvature analysis. If ratio $V_{\text{mod}}^{\text{min}}/V_{\text{analysis}}^{\text{max}} < 1$, the column is failed by shear, while if $V_{\text{mod}}^{\text{min}}/V_{\text{analysis}}^{\text{max}} > 1.2$, the column is failed by flexure. To avoid shear damage, the ratio $V_{\text{mod}}^{\text{min}}/V_{\text{analysis}}^{\text{max}} > 1.2$ is recommended to use in the design process.

Acknowledgment

This research is funded by Vietnam National Foundation for Science and Technology Development (NAFOSTED) under grant number 107.99-2017.316. The authors would like to thank Ms. Le Thi Thanh Tam for her contribution to this study.

References

[1] Yin, S. Y.-L., Wu, T.-L., Liu, T. C., Sheikh, S. A., Wang, R. (2011). Interlocking spiral confinement for rectangular columns. *ACI Concrete International*, 33(12):38–45.

[2] Dat, P. X., Vu, N. A. (2020). An experimental study on the structural performance of reinforced concrete low-rise building columns subjected to axial loading. *Journal of Science and Technology in Civil Engineering (STCE) - NUCE*, 14(1):103–111.

[3] Darwin, D., Dolan, C. W., Nilson, A. H. (2016). *Design of concrete structures*. 15th edition, McGraw-Hill, New York, USA.

[4] Wight, J. K. (1997). *Reinforced concrete: Mechanics and design*. 7th edition, Pearson Education, Upper Saddle River, New Jersey.

[5] Benzoni, G., Priestley, M. J. N., Seible, F. (2000). Seismic shear strength of columns with interlocking spiral reinforcement. In *12th World Conference on Earthquake Engineering, Auckland, New Zealand*.

[6] Correal, J. F., Saiidi, S., Sanders, D., El-Azazy, S. (2007). Shake table studies of bridge columns with double interlocking spirals. *ACI Structural Journal*, 104(4):393–401.

[7] McLean, D. I., Buckingham, G. C. (1994). *Seismic performance of bridge columns with interlocking spiral reinforcement*. Report No. WA-RD 357.1, Washington State Transportation Center, Washington, USA.

[8] Ou, Y.-C., Ngo, S.-H., Yin, S. Y., Wang, J.-C., Wang, P.-H. (2014). Shear Behavior of Oblong Bridge Columns with Innovative Seven-Spiral Transverse Reinforcement. *ACI Structural Journal*, 111(6):1339–1349.

[9] Igase, Y., Nomura, K., Kuroiwa, T., Miyagi, T. (2002). Seismic Performance and Construction Method of Bridge Columns with Interlocking Spiral/Hoop Reinforcement. *Concrete Journal*, 40(2):37–46.

[10] Wu, T.-L., Ou, Y.-C., Yin, S. Y.-L., Wang, J.-C., Wang, P.-H., Ngo, S.-H. (2013). Behavior of oblong and rectangular bridge columns with conventional tie and multi-spiral transverse reinforcement under combined axial and flexural loads. *Journal of the Chinese Institute of Engineers*, 36(8):980–993.

[11] Tanaka, H., Park, R. (1993). Seismic Design and Behavior of Reinforced Concrete Columns With Interlocking Spirals. *ACI Structural Journal*, 90(2):192–203.

[12] Ou, Y.-C., Ngo, S.-H., Roh, H., Yin, S. Y., Wang, J.-C., Wang, P.-H. (2015). Seismic Performance of Concrete Columns with Innovative Seven- and Eleven-Spiral Reinforcement. *ACI Structural Journal*, 112 (5):579–592.

[13] Nguyen, A. V., Pham, X. D. (2020). Experimental study on the structural performance of reinforced concrete columns subjected to axial loading. *Journal of Science and Technology in Civil Engineering, NUCE*, 14(2V):52–63. (in Vietnamese).

[14] Ang, B. G., Priestley, M. J. N., Paulay, T. (1989). Seismic Shear Strength of Circular Reinforced Concrete Columns. *ACI Structural Journal*, 86(1):45–59.

[15] AASHTO (2011). *AASHTO Guide Specifications for LRFD Seismic Bridge Design*. 2th edition. American Association of State Highway and Transportation Officials, Washington, DC, USA.

[16] Caltrans SDC (2019). *Seismic Design Criteria Version 2.0*. Engineering Service Center, Earthquake Engineering Branch, California, USA.

[17] Dancygier, A. N. (2001). Shear Carried by Transverse Reinforcement in Circular RC Elements. *Journal of Structural Engineering*, 127(1):81–83.

[18] Kim, J. H., Mander, J. B. (2005). Theoretical Shear Strength of Concrete Columns Due to Transverse Steel. *Journal of Structural Engineering*, 131(1):197–199.

[19] Jaafar, K. (2009). Discrete versus average integration in shear assessment of spiral links. *Canadian Journal of Civil Engineering*, 36(2):171–179.

[20] Ou, Y.-C., Ngo, S.-H. (2016). Discrete Shear Strength of Two- and Seven-Circular-Hoop and Spiral Transverse Reinforcement. *ACI Structural Journal*, 113(2):227–238.

[21] Ou, Y.-C., Ngo, S.-H. (2016). Discrete computational shear strength models for 5-, 6-, and 11-circular-hoop and spiral transverse reinforcement. *Advances in Structural Engineering*, 19(1):23–37.

[22] Priestley, M. J. N., Verma, R., Xiao, Y. (1994). Seismic Shear Strength of Reinforced Concrete Columns. *Journal of Structural Engineering*, 120(8):2310–2329.

[23] Sezen, H., Moehle, J. P. (2004). Shear Strength Model for Lightly Reinforced Concrete Columns. *Journal of Structural Engineering*, 130(11):1692–1703.

[24] Aschheim, M., Moehle, J. P. *Shear strength and deformability of RC bridge columns subjected to inelastic cyclic displacements*. Report No. UCB/EERC-92/04, Earthquake Engineering Research Center, University of California, Berkeley.

[25] Kowalsky, M. J., Priestley, M. J. N. (2000). Improved analytical model for shear strength of circular reinforced concrete columns in seismic regions. *ACI Structural Journal*, 97(3):388–396.